# Healing-block-assisted quasi-phase matching

Jui-Yu Lai,[1,2] Cheng-Wei Hsu,[1] Dong-Yi Wu,[2] Sheng-Bang Hung,[2] Ming-Hsien Chou,[2] and Shang-Da Yang[1,*]

[1]Institute of Photonics Technologies, National Tsing Hua University, Hsinchu 30013, Taiwan

[2]HC Photonics Corp., R&D Division, 4F, No. 2, Technology Rd. V, Hsinchu Science Park, Hsinchu 30078, Taiwan

*Corresponding author: shangda@ee.nthu.edu.tw

Received December 19, 2012; revised February 22, 2013; accepted February 26, 2013; posted February 27, 2013 (Doc. ID 182093); published April 1, 2013

A quasi-phase matching (QPM) structure based on phase correction by inserting a "healing block" (HB) of length $d_{\mathrm{HB}}$ into $M$ regular domains of constant length $d$ is proposed to enhance the nonlinear conversion efficiency when the first-order QPM domain length $d_1$ is too short to be reliably fabricated. Second-harmonic conversion efficiency 4.69 times higher than that of a third-order QPM grating has been experimentally demonstrated by using HB-QPM where all the domains are longer than $1.08d_1$. © 2013 Optical Society of America

*OCIS codes:* 230.4320, 160.3730, 190.2620.

The quasi-phase matching (QPM) technique [1] has been widely used in nonlinear wavelength conversion processes, for the utilization of the largest nonlinear tensor component enables much higher conversion efficiency over the birefringence phase matching (BPM) counterpart. In addition, the highly flexible QPM structures greatly facilitate some important applications. For example, fan-out and multiple QPM devices are useful in wavelength-tunable optical parametric oscillation (OPO) [2,3]. QPM gratings with spatially chirped periods are attractive in ultrafast wavelength conversion and pulse characterizations [4,5]. The cascaded QPM structure has been employed in the generation of a commensurate optical frequency comb and the synthesis of subfemtosecond waveforms [6]. Two-dimensional QPM permits an arbitrary conversion process in different spatial directions [7]. User-defined phase matching spectral grids can be realized by several optimization algorithms, such as genetic algorithms [8], and iterative domino [9]. However, the conversion efficiency of a real QPM device could be subject to the minimum domain length $d_{\min}$ that can be reliably fabricated. This is particularly evident when one of the operating wavelengths is close to the material absorption band, where the strong dispersion may result in a large wavevector mismatch $\Delta k$. For example, second-harmonic generation (SHG) of 914 nm using periodically poled 5 mol. % MgO-doped lithium niobate (PPMgLN) demands a short domain length of $d_1(=\pi/\Delta k) = 2.11$ μm to implement the first-order QPM [10]. In the event of $d_1 < d_{\min}$, a higher-order QPM structure is typically used at the cost of significantly reduced SHG efficiency. The second-order QPM with a 25/75 duty ratio can get the maximum SHG efficiency of $\eta_1/4$ ($\eta_1$ means the efficiency of the first-order QPM), but the smaller domain length remains $d_1$ [1]. As a consequence, the third-order QPM with an efficiency of $\eta_1/9$ is the common choice. It becomes highly desirable to access the large efficiency gap between $\eta_1$ and $\eta_1/9$, achieved by the first- and third-order QPM structures, respectively. In this Letter, we proposed and experimentally demonstrated the healing block (HB)-assisted QPM structure to address this issue for the first time (to the best of our knowledge). It is found that the SHG efficiency of HB-QPM could be higher than $\eta_1/9$ as long as $d_{\min} < 1.54d_1$. In our experiment, an HB-QPM structure with $d_{\min} = 1.08d_1$ achieved 4.69 times higher SHG efficiency than that of a third-order QPM grating of the same length.

Under the conditions of a plane wave and nondepleted pump, the SHG efficiency of an arbitrary QPM grating is

$$\eta = \eta_{\mathrm{norm}} \times |G|^2, \qquad G = \frac{1}{L}\int_0^L g(x)e^{i(\Delta k\cdot x)}\mathrm{d}x, \quad (1)$$

where $\eta_{\mathrm{norm}}$ is the normalized efficiency accounting for the input intensity, crystal nonlinearity, and grating length, $G$ is the complex mismatch function value, $g(x)$ denotes the $x$-dependent domain orientation, and $\Delta k$ is the wave vector mismatch. An HB-QPM grating consists of repeated substructures; each is composed of $M$ regular domains of constant length $d$ plus one longer HB of length $d_{\mathrm{HB}}$ [Fig. 1(a)]. The corresponding complex mismatch function value becomes

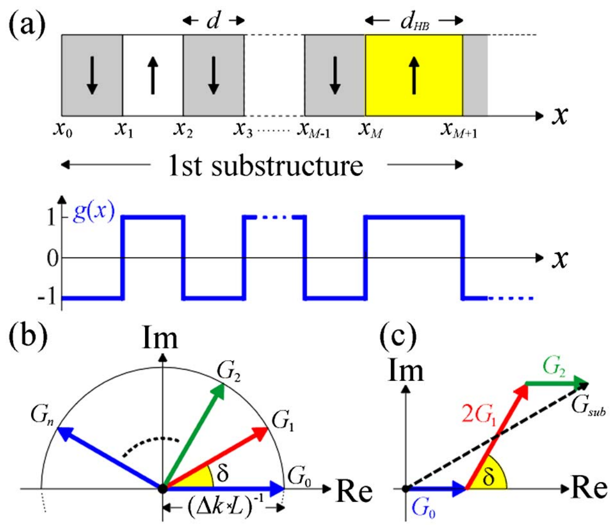


Fig. 1. (Color online) (a) Schematic of HB-QPM and the corresponding domain orientation distribution function $g(x)$, (b) the complex numbers $\{G_n\}$ contributed by uniformly spaced domain boundaries when the domain length $d$ is not an odd multiple of $d_1$, (c) the complex numbers $\{G_n\}$ and $G_{\mathrm{sub}}$ due to the individual domain boundaries (solid) and the entire substructure (dashed) with $M = 1$. All the following substructures will contribute to the same $G_{\mathrm{sub}}$ and can be added up constructively.

 

$$G = G_0 + G_N + 2\sum_{n=1}^{N-1} G_n, \qquad G_n = \frac{e^{i\phi_n}}{\Delta k \times L},$$
$$\phi_n = n\pi + \Delta k \times x_n, \tag{2}$$

where $N$ is the total number of domains. Equation (2) means that the $n$th domain boundary $x_n$ contributes to $G$ by a complex number $2G_n$ [except for the two end boundaries ($n = 0, N$), where the factor of "2" is absent]. In the case of the first-order QPM ($x_n = n \times d_1$, $\phi_n = 2n\pi$), $|G|$ is maximized, for all the constituent complex numbers $\{G_n\}$ are in-phased [$G_n = (\Delta k \times L)^{-1}$]. They remain perfectly in-phased in the third-order QPM ($x_n = n \times 3d_1$, $\phi_n = 4n\pi$), while the number of domains and the resulting $|G|$ are reduced by a factor of 3 compared with the first-order counterpart. For a uniform QPM with improper domain length $d = (1 + \Delta)d_1$, we got $x_n = n(1 + \Delta)d_1$, $\phi_n = n \times \delta$, and the complex numbers $G_n$, $G_{n-1}$ arising from two adjacent boundaries differ by a constant phase of $\delta = \Delta \times \pi$ [Fig. 1(b)]. As a result, $|G|$ is significantly reduced because of the mutual cancellation when summing up many complex numbers $\{G_n\}$ in Eq. (2). In HB-QPM, this problem is alleviated by reorienting the "vector" $G_{M+1}$ along the positive real axis (i.e., $\phi_{M+1}$ equals an integral multiple of $2\pi$) such that the complex mismatch function values $G_{\rm sub}$ due to individual substructures are identical and can be added up constructively. Figure 1(c) illustrates the idea by assuming only one regular domain ($M = 1$) per substructure.

For a general substructure with $M$ regular domains of length $(1 + \Delta)d_1$, the HB length $d_{\rm HB}$ is determined by having $\phi_{M+1} = 2(M + p + 1)\pi$ given $x_{M+1} = M(1 + \Delta)d_1 + d_{\rm HB}$. This will result in

$$d_{\rm HB} = (2p + 1 - M \times \Delta)d_1, \tag{3}$$

where $p$ is the smallest positive integer greater than $(M + 1)\Delta/2$ such that $d_{\rm HB} > d > d_1$ is satisfied. To formulate the SHG efficiency of an HB-QPM grating relative to that of a first-order QPM grating of the same length, one can employ Eq. (2) to calculate the corresponding complex mismatch function values

$$G_{\rm sub} = \frac{2e^{i(M\times\delta/2)}}{\Delta k \times L_{\rm sub}} \times \frac{\sin[(M+1)\delta/2]}{\sin(\delta/2)}, \quad G_{(1)} = \frac{2}{\pi},$$

where $L_{\rm sub} = M \times d + d_{\rm HB} = (M + 2p + 1)d_1$ represents the length of one substructure. As a result, the normalized SHG efficiency of an HB-QPM grating becomes

$$\mu = \left|\frac{G_{\rm sub}}{G_{(1)}}\right|^2 = \left\{\frac{1}{M + 2p + 1} \times \frac{\sin[(M+1)\delta/2]}{\sin(\delta/2)}\right\}^2. \tag{4}$$

The optimal number of $M$ for a given regular domain length $d = (1 + \Delta)d_1$ could be derived by maximizing Eq. (4). Figure 2(a) shows that the optimal number $M$ (solid curve) decreases with the increase of regular domain length $d$, for the phase difference $\delta$ increases with $d$ and will diminish $|G_{\rm sub}|$ [Fig. 1(c)]. Once the optimal $M$ is obtained, the corresponding HB length $d_{\rm HB}$ (dotted) is determined by Eq. (3). Figure 2(b) illustrates that the SHG efficiency of HB-QPM (solid curve) is higher than

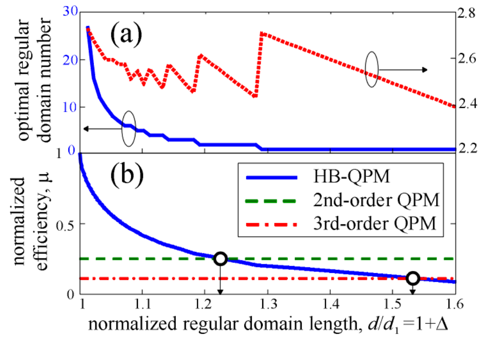


Fig. 2. (Color online) (a) Optimal number of regular domains (solid) and the corresponding normalized HB length $d_{\rm HB}/d_1$ (dotted), as well as (b) the normalized conversion efficiency $\mu$ (solid, achieved by using the optimal $M$ and $d_{\rm HB}$), as functions of the normalized regular domain length $d/d_1$. The efficiencies due to the second-order (dashed) and third-order (dashed–dotted) QPM are also shown for comparison.

those of the third-order (dashed–dotted curve) and second-order (dashed curve, assuming a duty cycle of 0.25) QPMs when the regular domain length is shorter than $1.54d_1$ and $1.23d_1$, respectively. As a result, the conversion efficiency gaps inherited by periodic QPM gratings can be sealed by using the HB-QPM structure.

A practical concern about QPM devices is the efficiency degradation due to overpoling or underpoling. A quantitative measure is the uniform overpoling ratio $r_{\rm op}$, defined by $d'_{\rm low} = (1 + r_{\rm op})d_{\rm low}$, where $d'_{\rm low}$ and $d_{\rm low}$ represent the actual and designed downward oriented domain lengths, respectively. Figure 3(a) shows that the conversion efficiency of a third-order QPM grating (dashed curve) will drop whenever the domains are overpoled ($r_{\rm op} > 0$) or underpoled ($r_{\rm op} < 0$). For HB-QPM

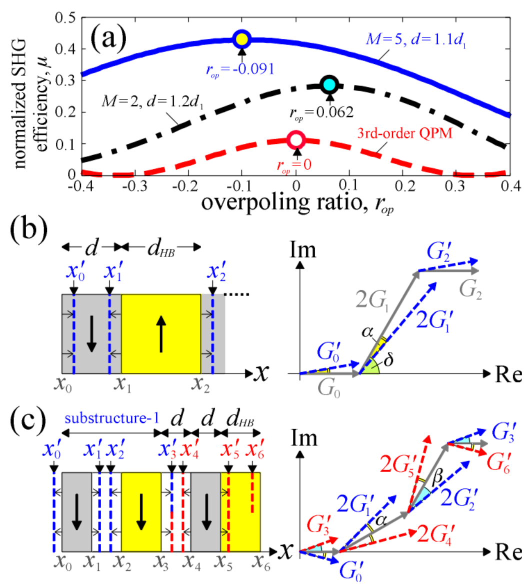


Fig. 3. (Color online) (a) Normalized SHG efficiencies versus the uniform overpoling ratio $r_{\rm op}$ for third-order QPM (dashed) and HB-QPM with an odd (solid) and even (dashed–dotted) number of regular domains. Schematic and complex numbers $\{G_n\}$, $\{G'_n\}$ of HB-QPM structures with (b) underpoling, one regular domain, and (c) overpoling, two regular domains, respectively.

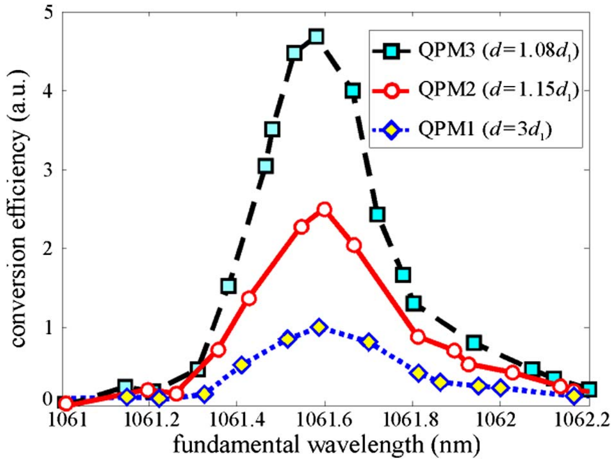


Fig. 4. (Color online) Experimentally measured phase matching tuning curves of QPM1 (diamonds), QPM2 (circles), and QPM3 (squares), respectively.

with an odd number of regular domains [Fig. 3(b), $M = 1$], all the downward oriented domains are regular ones. The complex numbers $G'_n$, $G_n$ contributed by the actual and designed domain boundaries $x'_n$, $x_n$ will differ by a phase of $\alpha = \pm r_{\rm op}(\pi + \delta)/2$. A slightly underpoled HB-QPM structure may give a larger $|G'_{\rm sub}|$, for the relative phase shift between $G'_n$ and $G'_{n-1}$ ($n \in$ odd) is reduced to $\delta - 2\alpha$. Maximum conversion efficiency occurs when $\delta = 2\alpha$, i.e., $r_{\rm op} = -\delta/(\pi + \delta)$ [Fig. 3(a), solid curve]. In contrast, the efficiency of an HB-QPM structure with an even number of regular domains is peaked in the presence of slight overpoling [Fig. 3(a), dashed–dotted curve]. In this case, $G_{\rm sub}$ will repeat itself for every two substructures, for the twoHBs are oriented oppositely. For the specific case of $M = 2$ and $r_{\rm op} > 0$ [Fig. 3(c)], the enlarged HB within $(x'_2, x'_3)$ contributes to $G'_2$, $G'_3$ with a different phase shift $\pm\beta$ with respect to $G_2$, $G_3$ (while all the other $G'_n$ still differ from $G_n$ by a phase of $\pm\alpha$). It can be shown that $|G'_{\rm sub}| > |G_{\rm sub}|$ occurs when

$$\cos\alpha + \cos(\delta - \beta) + \cos(\delta + \alpha) > 1 + 2\cos\delta \quad (\text{if } M = 2).$$

In a proof-of-concept experiment, we fabricated an 8 mm long PPMgLN chip with three different QPM gratings designed for frequency doubling of 1064 nm ($d_1 = 3.46$ μm). The first grating (QPM1) is a third-order QPM with a constant domain length of $3d_1 = 10.38$ μm. The other two gratings are designed by HB-QPM, where QPM2 and QPM3 are with $M = 3$, $d = 4.00$ μm $(1.15d_1)$, $d_{\rm HB} = 8.76$ μm $(2.53d_1)$, and $M = 5$, $d = 3.75$ μm $(1.08d_1)$, $d_{\rm HB} = 8.93$ μm $(2.58d_1)$, respectively. A beam at ~1064 nm from a wavelength-tunable CW laser is focused into a QPM grating of the PPMgLN chip for frequency doubling. The temperature is slightly tuned ($28 \pm 1$°C) to precisely determine the peak conversion efficiency at the central wavelength of 1061.6 nm. Two dichroic mirrors are used to suppress the residual fundamental power, and the second-harmonic power is measured by a photodetector. Figure 4 illustrates the experimentally measured phase matching tuning curves of the three QPM gratings. The peak conversion efficiencies of QPM2 (circles) and QPM3 (squares) are 2.50 and 4.69 times higher than that of QPM1 (diamonds), which are in good agreement with the theoretical values of 2.95 and 4.16, respectively. The error could arise from the random duty cycle error during the fabrication processes.

In summary, we proposed and experimentally demonstrated the HB-QPM structure to enhance the conversion efficiency when the first-order QPM domain length $d_1$ is too short to be reliably fabricated. Our calculation showed that efficiency enhancement over the third-order QPM occurs if the regular domain length is shorter than $1.54d_1$. In our experiments, the SHG efficiency of HB-QPM could be 4.69 (2.50) times higher than that achieved by the third-order QPM if the regular domain length $d$ is 1.08 (1.15) times the value of $d_1$. HB-QPM is simple, robust against the uniform overpoling/underpoling error, and particularly useful in high-power, short-wavelength conversion processes where short-period poling over thick nonlinear crystal is typically challenging.

This material is based on research supported by the National Science Council in Taiwan under grants NSC 100-2221-E-007-093-MY3 and 99-2120-M-007-010 and by the National Tsing Hua University under grant 100N2081E1.

## References

1. M. M. Fejer, G. A. Magel, D. H. Jundt, and R. L. Byer, IEEE J. Quantum Electron. **28**, 2631 (1992).
2. P. E. Powers, T. J. Kulp, and S. E. Bisson, Opt. Lett. **23**, 159 (1998).
3. L. E. Myers, R. C. Eckardt, M. M. Fejer, R. L. Byer, and W. R. Bosenberg, Opt. Lett. **21**, 591 (1996).
4. C. Heese, C. R. Phillips, L. Gallmann, M. M. Fejer, and U. Keller, Opt. Lett. **35**, 2340 (2010).
5. S.-D. Yang, A. M. Weiner, K. R. Parameswaran, and M. M. Fejer, Opt. Lett. **30**, 2164 (2005).
6. H. Chan, Z. Hsieh, L. Peng, and A. H. Kung, Opt. Lett. **37**, 2805 (2012).
7. R. Lifshitz, A. Arie, and A. Bahabad, Phys. Rev. Lett. **95**, 133901 (2005).
8. J.-Y. Lai, Y.-J. Liu, H.-Y. Wu, Y.-H. Chen, and S.-D. Yang, Opt. Express **18**, 5328 (2010).
9. J.-Y. Lai, C.-W. Hsu, N. Hsu, Y.-H. Chen, and S.-D. Yang, Opt. Lett. **37**, 1184 (2012).
10. O. Gayer, Z. Sacks, E. Galun, and A. Arie, Appl. Phys. B. **91**, 343 (2008).